

Gluon saturation in pA collisions at energies available at the CERN Large Hadron Collider: Predictions for hadron multiplicities

Adrian Dumitru,^{1,2} Dmitri E. Kharzeev,^{3,4} Eugene M. Levin,^{5,6} and Yasushi Nara⁷

¹*RIKEN BNL Research Center, Brookhaven National Laboratory, Upton, New York 11973, USA*

²*Department of Natural Sciences, Baruch College, CUNY, 17 Lexington Avenue, New York, New York 10010, USA*

³*Department of Physics and Astronomy, Stony Brook University, Stony Brook, New York 11794, USA*

⁴*Department of Physics, Brookhaven National Laboratory, Upton, New York 11973, USA*

⁵*Department of Particle Physics, School of Physics and Astronomy, Tel Aviv University, 69978 Tel Aviv, Israel*

⁶*Departamento de Física, Centro de Estudios Subatómicos, Universidad Técnica Federico Santa María, and Centro Científico-Tecnológico de Valparaíso, Casilla 110-V, Valparaíso, Chile*

⁷*Akita International University, Yuwa, Akita-city 010-1292, Japan*

(Received 14 December 2011; published 20 April 2012)

The upcoming $p + \text{Pb}$ run at the Large Hadron Collider (LHC) will probe the nuclear gluon distribution at very small Bjorken x (from $x \sim 10^{-4}$ at midrapidity down to $x \sim 10^{-6}$ in the proton fragmentation region) and will allow testing of approaches based on parton saturation. Here, we present the predictions of the Kharzeev-Levin-Nardi model for hadron multiplicities and multiplicity distributions in $p + \text{Pb}$ collisions at a center-of-mass energy of 4.4 TeV. We also compare the model to the existing pp , dA , and AA data from the Relativistic Heavy Ion Collider and LHC.

DOI: [10.1103/PhysRevC.85.044920](https://doi.org/10.1103/PhysRevC.85.044920)

PACS number(s): 25.75.Ag

I. INTRODUCTION

Very soon, the Large Hadron Collider (LHC) will record the first data on $p + \text{Pb}$ collisions at the center-of-mass energy of 4.4 TeV. These data will allow the nuclear gluon distributions to be probed at very small Bjorken x : from $x \sim 10^{-4}$ at midrapidity down to $x \sim 10^{-6}$ in the proton fragmentation region. Because the QCD evolution makes parton distributions increase at small x , the LHC experiments will allow the nuclear wave functions to be probed at unprecedented parton densities. These measurements are crucial for testing the current theoretical approaches to high-energy QCD.

Owing to the breaking of scale invariance by quantum effects, QCD possesses a dimensionful scale Λ_{QCD} that determines the characteristic distance $\sim \Lambda_{\text{QCD}}^{-1}$ at which the dynamics becomes nonperturbative. The asymptotic freedom [1,2] makes the perturbative expansion valid only if a hard external scale $Q^2 \gg \Lambda_{\text{QCD}}^2$ is present. Multiparticle production in hadron collisions is dominated by soft interactions and so in general is not amenable to the weak-coupling treatment. However, when the density of partons in the transverse plane Q_s^2 becomes large compared to Λ_{QCD}^2 , it regularizes the infrared behavior of the parton transverse momentum distributions at the “saturation momentum” [3] Q_s and thus prevents the running coupling of QCD from growing large: $\alpha_s(Q_s) = g^2/4\pi \ll 1$ [3–5]. The gluon field A in this weak-coupling regime has a large occupation number, $A \sim 1/g > 1$, and can be treated as a classical “color glass condensate” [5–7].

Although the complete theory of multiparticle production based on the ideas outlined above is still being developed, its main ingredients are clear and can serve as the basis for phenomenology. This was the motivation for the Kharzeev-Levin-Nardi (KLN) model [8–10] combining the Glauber approach to proton-nucleus and nucleus-nucleus collisions

(for a complete set of formulas see, e.g., Ref. [11]) with a simple ansatz for the unintegrated parton distributions that accounts for the existence of a new dimensionful scale—the saturation momentum. The KLN model was successful in describing the Relativistic Heavy Ion Collider (RHIC) data [12–15] on the centrality and rapidity dependence of charged-hadron production in heavy-ion collisions. The predictions for Pb-Pb and p -Pb collisions at the LHC were made in Ref. [16]. The comparison to the first LHC data [17] on hadron production in Pb-Pb collisions revealed that, whereas the KLN model describes the centrality dependence rather well, the overall normalization exceeds the observed one by about 10–15%. This implies that the energy dependence of the saturation momentum assumed in Ref. [16] was slightly too steep.¹

Regarding pA collisions, we also have to remember that the number of “participants” (the nucleons that underwent at least one inelastic interaction) in this case is much smaller than in A - A collisions, and that fluctuations are much more important. Therefore, a Monte Carlo (MC)–based formulation [18] of the numerical integration of the KLN model [19] can be expected to provide more accurate predictions. Indeed, the MC method leads to a better agreement between the data and the model prediction [20] in d - Au collisions at RHIC. The MC-based KLN model [18] has been used to generate initial conditions for the hydrodynamical description of collective flow (see, e.g., Refs. [21–23]).

¹While it is evident that the model has to be refined, let us put this discrepancy in perspective by noting that some of the early pre-RHIC predictions for the LHC that did not take into account the concepts of parton saturation and coherence overestimated the measured hadron multiplicity by almost an order of magnitude.

The goal of this paper is to provide updated predictions for p -Pb collisions at the LHC. Let us explicitly list the differences between the present and the previous [16] papers: (i) we consider the center of mass system (c.m.s.) energy of the forthcoming p -Pb run, 4.4 TeV; (ii) we reduced the intercept describing the energy dependence of saturation momentum by $\sim 20\%$; and (iii) we employ the MC method of evaluating the number of participants. Of course, after making these changes we have to make sure that the RHIC data are still adequately described; therefore, we present the comparison to the RHIC AA and dA as well. While these changes may seem insignificant, the p -Pb LHC data present a chance to test saturation ideas, and this requires quantitative predictions made to the best of our current knowledge.

II. THE KLN MODEL

Let us briefly recall the basic ingredients of the KLN approach; for details, see Refs. [9,16]. The multiplicity per unit rapidity,

$$\frac{dN}{dy} = \frac{K}{S} \int dp_t^2 \left(E \frac{d\sigma}{d^3p} \right) = \frac{K}{S} \frac{4\pi N_c \alpha_s}{N_c^2 - 1} \times \int_0^\infty \frac{d p_t^2}{p_t^4} x_2 G_{A_2}(x_2, p_t^2) x_1 G_{A_1}(x_1, p_t^2), \quad (1)$$

is evaluated using the gluon density obtained from a simple ansatz for the unintegrated gluon distribution [9] encoding the saturation phenomenon:

$$xG(x, p_t^2) = \begin{cases} \frac{S}{\alpha_s(Q_s)} p_t^2 (1-x)^4, & p_t < Q_s(x), \\ \frac{S}{\alpha_s(Q_s)} Q_s^2 (1-x)^4, & p_t > Q_s(x), \end{cases} \quad (2)$$

where $x = x_1$ or x_2 , with $x_{1,2} = (p_t/W)e^{\pm y}$; the $+$ ($-$) sign in the exponent applies to the projectile (target), and $W \equiv \sqrt{s}$ is the c.m.s. energy. The factor S in Eq. (1) is the transverse area involved in the collision (see below). The normalization factor K describes the conversion of partons to hadrons and is determined by a global fit to pp data at various energies, and to $d + Au$ data from RHIC.

To describe the running of QCD coupling, we use the β function in the one-loop approximation with $N_f = 3$ light quark flavors and $\Lambda_{\text{QCD}}^2 = 0.05 \text{ GeV}^2$ but we assume that the coupling freezes at $\alpha_{\text{max}} = 0.52$ [24]:

$$\alpha_s(Q^2) = \min \left[\frac{12\pi}{27 \ln \frac{Q^2}{\Lambda_{\text{QCD}}^2}}, \alpha_{\text{max}} \right], \quad (Q^2 \geq \Lambda_{\text{QCD}}^2). \quad (3)$$

The factor of $\alpha_s(Q^2)$ in integral (1) is evaluated at the scale p_t^2 , if this is the largest scale, or else at the lower of $Q_s^2, p(y)$ or $Q_{s,T}^2(y)$. The saturation momenta are defined as

$$Q_s^2(y) = Q_0^2 N_{\text{part}} \left(x_0 \frac{W}{Q_0} e^{\mp y} \right)^{\bar{\lambda}}, \quad (4)$$

where again the $+$ ($-$) sign in the exponent applies to the projectile (target). We fix the parameters to $Q_0 = 0.6 \text{ GeV}$, $x_0 = 0.01$, and $\bar{\lambda} = 0.205$. In the midrapidity region of

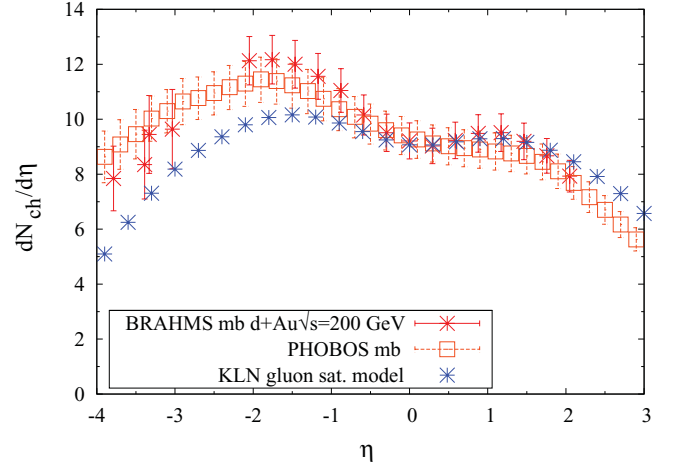


FIG. 1. (Color online) Rapidity distribution of charged particles in minimum-bias $d + Au$ collisions at $W = 200 \text{ GeV}$. PHOBOS and BRAHMS data from Refs. [27,28].

collisions at RHIC energy, this results in a gluon saturation momentum $Q_s \simeq 0.68 \text{ GeV}$ for a proton. On account of the large radius of the deuteron, we have used $N_{\text{part},P} = 1$ in Eq. (4) in this case assuming that the parton substructure of the nucleon in the deuteron is not modified. For minimum-bias $d + Au$ collisions we multiply dN/dy by a factor of 1.52, which is our estimate for the corresponding equivalent number of $p + Au$ collisions at an energy of $W = 200 \text{ GeV}$. For pp collisions we choose the effective area $S_{pp} \simeq 0.7 S_{pA}$, somewhat smaller than for pA collisions, as suggested by the data. This may be an indication that in proton-proton collisions only part of the proton takes part in the interaction. However, the large nucleus makes all of the proton's constituents interact.

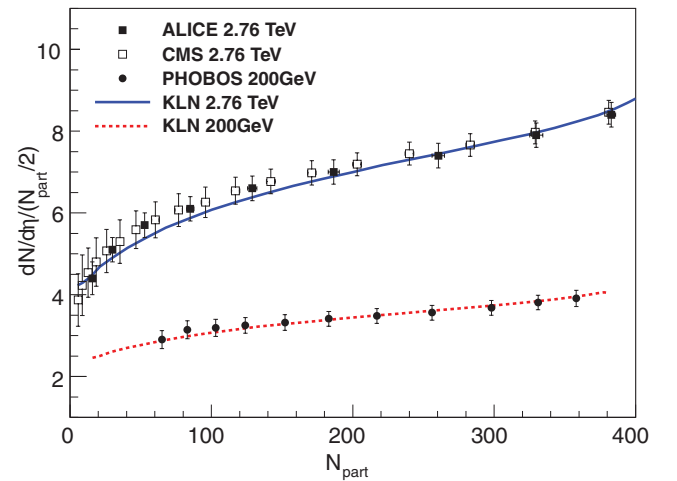


FIG. 2. (Color online) Centrality dependence of the charged-hadron multiplicity at $\eta = 0$ in Au + Au collisions at $W = 200 \text{ GeV}$ [14] and Pb + Pb collisions at $W = 2.76 \text{ TeV}$ [17,29].

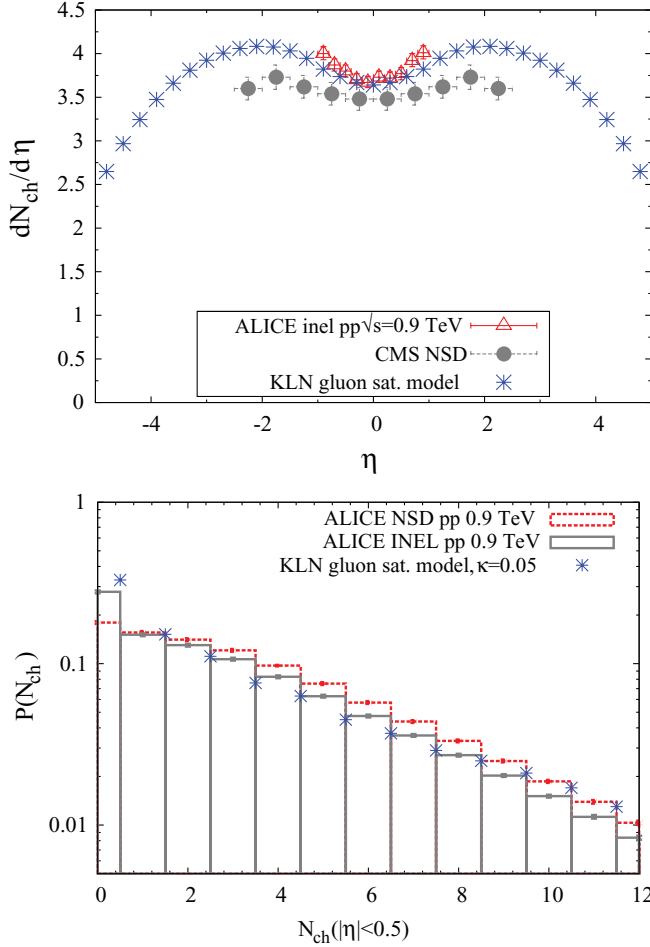


FIG. 3. (Color online) Top: Rapidity distribution of charged particles in pp collisions at $W = 900$ GeV. Bottom: Charged-particle multiplicity distribution. ALICE and CMS data from Refs. [30,31].

To evaluate the pseudorapidity distributions, Eq. (1) needs to be rewritten using the transformation

$$y(\eta) = \frac{1}{2} \ln \frac{\sqrt{\cosh^2 \eta + \mu^2} + \sinh \eta}{\sqrt{\cosh^2 \eta + \mu^2} - \sinh \eta} \quad (5)$$

with the Jacobian

$$J(\eta) = \frac{\partial y}{\partial \eta} = \frac{\cosh \eta}{\sqrt{\cosh^2 \eta + \mu^2}}. \quad (6)$$

The scale $\mu^2(W)$ is allowed to exhibit a weak energy dependence according to

$$\mu(W) = \frac{0.24}{0.13 + 0.32 W^{0.115}}, \quad (7)$$

with W expressed in units of TeV. This parametrization reproduces approximately the ‘‘shoulder’’ structure of $dN/d\eta$ observed in symmetric pp collisions. We did not modify $\mu(W)$ for the case of pA collisions.

The multiplicity discussed above represents the *average* multiplicity $\langle N_{\text{ch}} \rangle$ observed in collisions with a fixed number of participants. In experiment, the multiplicity fluctuates both due to the fluctuations in the number of participants and due

to ‘‘intrinsic’’ fluctuation at a fixed number of participants. To model the intrinsic fluctuations of the number of produced particles, we consider the multiplicity (per unit rapidity) as a random variable distributed according to a negative binomial distribution,

$$P(N_{\text{ch}}) = \frac{\Gamma(k+n)}{\Gamma(k)\Gamma(n+1)} \frac{\langle N_{\text{ch}} \rangle^{N_{\text{ch}}} k^k}{(\langle N_{\text{ch}} \rangle + k)^{N_{\text{ch}}+k}}. \quad (8)$$

The quantity k which characterizes the fluctuations in the saturation approach has been estimated as be [25,26]

$$k = \kappa \frac{N_c^2 - 1}{2\pi} Q_s^2(y, W) \sigma_k(W). \quad (9)$$

In our numerical estimates we assumed that $\sigma_k(W) = \sigma_{\text{in}}(W)/10$ is proportional to the inelastic pp cross section and that Q_s is the saturation scale of the proton. We find that the value of κ that describes best the multiplicity distributions in pp collisions is about $\kappa \simeq 0.05$.

All observables for pA collisions finally need to be averaged also over an ensemble of $N_{\text{part},A}$, which enters through Eq. (4). We obtain the number of participants in the

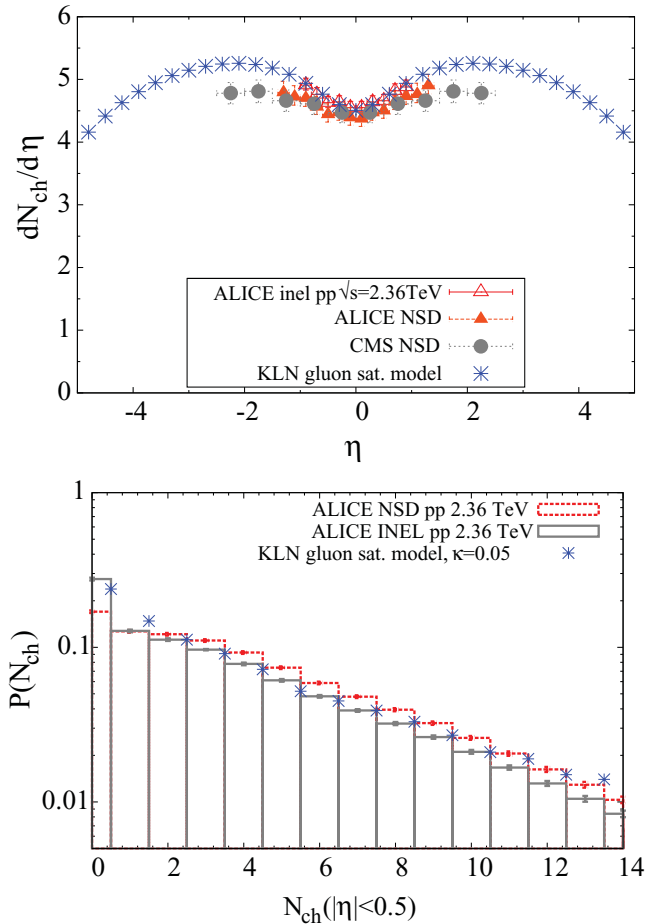


FIG. 4. (Color online) Top: Rapidity distribution of charged particles in pp collisions at $W = 2360$ GeV. Bottom: Charged-particle multiplicity distribution. ALICE and CMS data from Refs. [30,31].

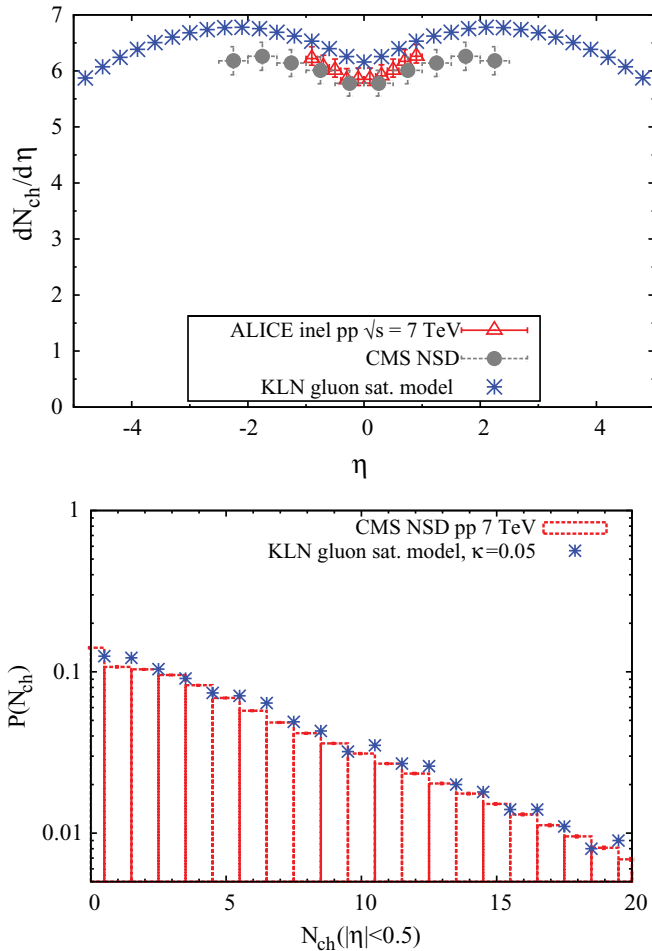


FIG. 5. (Color online) Top: Rapidity distribution of charged particles in pp collisions at $W = 7000$ GeV. Bottom: Charged-particle multiplicity distribution. ALICE and CMS data from Refs. [30,31].

heavy-ion target from a Monte Carlo Glauber simulation²: assume a uniformly distributed random number $0 < \nu < 1$ and let

$$N_{part,A}(\vec{b}) = \sum_{i=1,\dots,A} \Theta(P(\vec{b} - \vec{r}_i) - \nu_i). \quad (10)$$

Here, b is the impact parameter of the $p + A$ collision, i.e., the transverse distance of the proton from the center of the target nucleus; it is a random variable with the probability density $b db$. The set $\{\vec{r}_i\}$ corresponds to the coordinates of the nucleons in the target which are picked randomly according to a Woods-Saxon distribution. Finally, $P(r)$ denotes the interaction probability of two nucleons separated by a transverse distance r ; for simplicity, here we assume “hard

²However, in AA collisions the fluctuations of N_{part} do not affect the multiplicity strongly; we have calculated N_{part} directly, in a “mean-field approximation,” from a nuclear Woods-Saxon distribution.

sphere” nucleons:

$$P(r) = \Theta\left(\sqrt{\frac{\sigma_{in}(W)}{\pi}} - r\right). \quad (11)$$

We use the measured values $\sigma_{in}(s) = 42, 52, 60, 65.75,$ and 70.45 mb at $W = 200, 900, 2360, 4400,$ and 7000 GeV, respectively.

III. RESULTS AND DISCUSSION

Let us now present and describe our results. First we recheck the model against the RHIC data. Figure 1 shows the comparison to the d -Au data; in the range $-1 < \eta < 2$ the agreement is satisfactory. Note that at $\eta \gtrsim 2$ the saturation momentum of the projectile becomes small and so the validity of the saturation approach is questionable at best. Also, in the fragmentation region of the nucleus one would have to account for the contribution from valence quarks to improve agreement with the data.

The centrality dependence of the charged-particle multiplicity in Au+Au collisions at RHIC is shown in Fig. 2; the

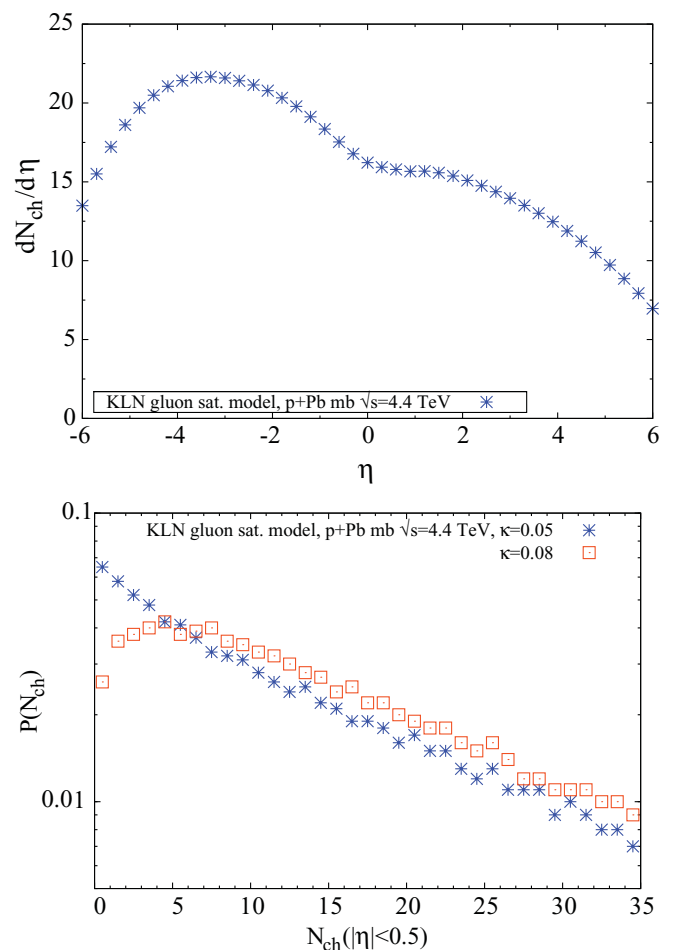


FIG. 6. (Color online) Top: Rapidity distribution of charged particles in minimum-bias $p + Pb$ collisions at $W = 4400$ GeV. An $\sim 10\%$ overall normalization uncertainty is not shown explicitly. Bottom: Charged-particle multiplicity distribution.

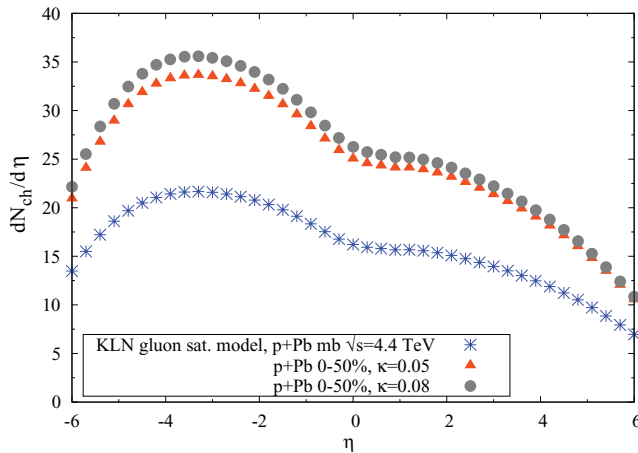


FIG. 7. (Color online) Rapidity distribution of charged particles in $p + \text{Pb}$ collisions at $W = 4400$ GeV for minimum-bias trigger and for the 0–50 % centrality or multiplicity class. An $\sim 10\%$ overall normalization uncertainty is not shown explicitly.

agreement is very good. The reduction of the intercept of the gluon distribution (by $\sim 20\%$ in comparison with Ref. [16]) allows us to reproduce well also the LHC Pb+Pb data (see Fig. 2). Figures 3, 4, and 5 show the comparison of our model to the pp data from the LHC on charged-hadron multiplicities and multiplicity distributions at $\sqrt{s} = 0.9, 2.36,$ and 7 TeV, respectively. The agreement is seen to be quite good. Finally, in Figs. 6 and 7 we present our predictions for the upcoming p -Pb run at $\sqrt{s} = 4.4$ TeV.

To summarize, we presented updated predictions of the KLN model for p -Pb collisions at the LHC, as well as comparisons to the RHIC and LHC data on hadron multiplicities and multiplicity distributions. Clearly, our treatment has been somewhat model dependent and involves a few adjustable parameters. Nevertheless, our model does capture the emergence of a new dimensionful scale governing QCD interactions at high energies and thus expresses in quantitative form the essence of the parton saturation phenomenon. The comparison of our model to the existing Pb-Pb and the forthcoming p -Pb data would also allow us to deduce the amount of additional entropy produced during the evolution of the quark-gluon fluid in heavy-ion collisions [32]. Our present treatment assumes no additional entropy production, which corresponds to the zero-viscosity limit; a deviation from our prediction could signal the presence of viscous effects.

ACKNOWLEDGMENTS

A.D. gratefully acknowledges support by the DOE Office of Nuclear Physics through Grant No. DE-FG02-09ER41620 and by The City University of New York through the PSC-CUNY Research Award Program, Grant No. 64132-0042. The work of D.K. was supported in part by the US Department of Energy under Contracts No. DE-AC02-98CH10886 and No. DE-FG-88ER41723. The work of E.L. was supported in part by the Fondecyt (Chile) Grant No. 1100648. The work of Y.N. was partly supported by Grant-in-Aid for Scientific Research No. 20540276.

-
- [1] D. J. Gross and F. Wilczek, *Phys. Rev. Lett.* **30**, 1343 (1973).
[2] H. D. Politzer, *Phys. Rev. Lett.* **30**, 1346 (1973).
[3] L. V. Gribov, E. M. Levin, and M. G. Ryskin, *Phys. Rep.* **100**, 1 (1983).
[4] A. H. Mueller and J. Qiu, *Nucl. Phys. B* **268**, 427 (1986); J.-P. Blaizot and A. H. Mueller, *ibid.* **289**, 847 (1987).
[5] L. McLerran and R. Venugopalan, *Phys. Rev. D* **49**, 2233 (1994); **49**, 3352 (1994); **50**, 2225 (1994).
[6] I. A. Balitsky, *Nucl. Phys. B* **463**, 99 (1996); Y. V. Kovchegov, *Phys. Rev. D* **60**, 034008 (1999).
[7] J. Jalilian-Marian, A. Kovner, A. Leonidov, and H. Weigert, *Phys. Rev. D* **59**, 014014 (1998); *Nucl. Phys. B* **504**, 415 (1997); E. Iancu, A. Leonidov, and L. D. McLerran, *Phys. Lett. B* **510**, 133 (2001); *Nucl. Phys. A* **692**, 583 (2001); H. Weigert, *ibid.* **703**, 823 (2002).
[8] D. Kharzeev and M. Nardi, *Phys. Lett. B* **507**, 121 (2001).
[9] D. Kharzeev and E. Levin, *Phys. Lett. B* **523**, 79 (2001).
[10] D. Kharzeev, E. Levin, and M. Nardi, *Phys. Rev. C* **71**, 054903 (2005).
[11] D. Kharzeev, C. Lourenco, M. Nardi, and H. Satz, *Z. Phys. C* **74**, 307 (1997).
[12] I. G. Bearden (BRAHMS Collaboration), *Phys. Rev. Lett.* **87**, 112305 (2001); **88**, 202301 (2002); *Phys. Lett. B* **523**, 227 (2001).
[13] A. Bazilevsky (PHENIX Collaboration), *Nucl. Phys. A* **715**, 486 (2003); A. Milov (PHENIX Collaboration), *ibid.* **698**, 171 (2002); K. Adcox *et al.* (PHENIX Collaboration), *Phys. Rev. Lett.* **87**, 052301 (2001); **86**, 3500 (2001).
[14] B. B. Back *et al.* (PHOBOS Collaboration), *Phys. Rev. Lett.* **85**, 3100 (2000); *Phys. Rev. C* **65**, 061901 (2002); *Phys. Rev. Lett.* **87**, 102303 (2001); **85**, 3100 (2000).
[15] Z. b. Xu (STAR Collaboration), *arXiv:nucl-ex/0207019*; C. Adler *et al.* (STAR Collaboration), *Phys. Rev. Lett.* **87**, 112303 (2001).
[16] D. Kharzeev, E. Levin, and M. Nardi, *Nucl. Phys. A* **747**, 609 (2005).
[17] K. Aamodt *et al.* (ALICE Collaboration), *Phys. Rev. Lett.* **106**, 032301 (2011).
[18] H.-J. Drescher and Y. Nara, *Phys. Rev. C* **75**, 034905 (2007); **76**, 041903(R) (2007).
[19] A. Adil, H.-J. Drescher, A. Dumitru, A. Hayashigaki, and Y. Nara, *Phys. Rev. C* **74**, 044905 (2006).
[20] D. Kharzeev, E. Levin, and M. Nardi, *Nucl. Phys. A* **730**, 448 (2004).
[21] T. Hirano, U. W. Heinz, D. Kharzeev, R. Lacey, and Y. Nara, *Phys. Lett. B* **636**, 299 (2006).
[22] T. Hirano and Y. Nara, *Phys. Rev. C* **79**, 064904 (2009).
[23] H. Song, S. A. Bass, U. Heinz, T. Hirano, and C. Shen, *Phys. Rev. Lett.* **106**, 192301 (2011).

- [24] Y. L. Dokshitzer, *Acta Phys. Pol. B* **36**, 361 (2005).
- [25] F. Gelis, T. Lappi, and L. McLerran, *Nucl. Phys. A* **828**, 149 (2009).
- [26] P. Tribedy and R. Venugopalan, *Nucl. Phys. A* **850**, 136 (2011).
- [27] B. B. Back *et al.* (PHOBOS Collaboration), *Phys. Rev. C* **72**, 031901 (2005).
- [28] I. Arsene *et al.* (BRAHMS Collaboration), *Phys. Rev. Lett.* **94**, 032301 (2005).
- [29] S. Chatrchyan *et al.* (CMS Collaboration), *J. High Energy Phys.* **8** (2011) 141.
- [30] K. Aamodt *et al.* (ALICE Collaboration), *Eur. Phys. J. C* **65**, 111 (2010); **68**, 89 (2010); **68**, 345 (2010).
- [31] V. Khachatryan *et al.* (CMS Collaboration), *J. High Energy Phys.* **1002** (2010) 041; **1101** (2011) 079.
- [32] A. Dumitru, E. Molnar, and Y. Nara, *Phys. Rev. C* **76**, 024910 (2007).